# Observation of Resonance Soliton Trapping due to a Photoinduced Gap in Wave Number

G. Van Simaeys,[1] S. Coen,[1] M. Haelterman,[1] and S. Trillo[2,3]

[1]*Service d'optique et d'acoustique, Université Libre de Bruxelles, 50 Avenue F. D. Roosevelt, CP 194/5, 1050 Brussels, Belgium*

[2]*Department of Engineering, University of Ferrara, Via Saragat 1, 44100 Ferrara, Italy*

[3]*INFM-RM3, Via della Vasca Navale 84, 00146 Roma, Italy*

(Received 16 July 2003; published 2 June 2004)

We investigate the nonlinear propagation of two forward propagating modes coupled by a resonant traveling-wave grating, which is photoinduced by illuminating an optical fiber with a beat signal. This interaction, representative of systems whose dispersion relation $K = K(\Omega)$ exhibits a gap in momentum $K$, shows evidence of localization mediated by resonance solitons. The signature of a still (in the grating frame) soliton is grating-induced cancellation of modal group-velocity mismatch.

DOI: 10.1103/PhysRevLett.92.223902 PACS numbers: 42.65.Tg, 03.50.De, 05.45.Yv, 42.65.Jx

The nonlinear response of structures engineered in periodic fashion allows one to control the flow of light [1–3]. Of growing importance are photonic band gap structures, so-called because stop bands (gaps) in *frequency* $\Omega$ (or energy) appear in their linear dispersion relation. In 1D Bragg coupling, the most elementary of these structures, an intensity-dependent index, makes the propagation at frequencies inside (or outside but close to) the gap allowed in the form of gap solitons (GSs) [4–6], localized envelopes that can be stable while traveling in principle with any velocity lower than light velocity. Relying on the interplay of periodicity and nonlinearity, this concept is ubiquitous [7] and goes beyond specific nonlinear mechanisms [8] and system dimensionality [9]. Optical fibers or AlGaAs guides with permanently built-in Bragg gratings have been proven to be ideal test beds for the physics of GSs [1,2]. Yet, to date the strong reflectivity of such gratings has prevented the experimental exploration of the physics deep inside the gap (e.g., approaching the resonance) and/or the excitation of still GSs.

While Bragg coupling occurs between waves propagating in opposite directions [backward coupling (BWC)], gratings with longer pitch can be resonant also with copropagating modes leading to forward coupling (FWC) [10]. The possibility that nonlinear trapping occurs in the latter situation has long been overlooked, in spite of the fact that so-called *resonance solitons* have been pointed out to exist, owing to grating-assisted FWC, in the context of early studies of GSs [11]. In this Letter we report the first evidence of resonance soliton trapping showing their universal nature of localized states associated with a *gap in wave number* (or momentum, $K$ gap). To this end, we exploit a traveling-wave (henceforth, *dynamic*) *light-induced* grating characterized by a $K$ gap [12] instead of $\Omega$ gaps of permanent Bragg gratings. Our resonant grating originates from the nonlinear response (rather than photosensitivity or photorefraction [3]) of a standard fiber and permits overcoming the drawbacks of other grating-assisted FWC schemes [10]. Because of the features of FWC occurring in this dynamic grating, we observe trapping right on-resonance (gap center), in sharp contrast with all experiments conducted so far on GSs in static Bragg gratings.

In our arrangement, FWC occurs between two beating signal frequencies owing to another dual-color resonant (same beat frequency) grating wave copropagating along the same optical fiber. The intensity modulation associated with the latter induces, through nonlinear cross-phase modulation, a traveling-wave periodic index change (the dynamic grating). For slow modulations, the interaction of the grating wave envelope $E_g(Z, T)$ at carrier frequency $\omega_g$ and the signal wave $E_s(Z, T)$ (carrier $\omega_s$) can be described with sufficient accuracy by the nonlinear Schrödinger equations (NLSEs) [13]

$$\begin{aligned} &i\partial_Z E_g - (k_g''/2)\partial_T^2 E_g + \chi(|E_g|^2 + 2|E_s|^2)E_g = 0, \\ &i(\partial_Z + \delta\partial_T)E_s - (k_s''/2)\partial_T^2 E_s + \chi(|E_s|^2 + 2|E_g|^2)E_s = 0, \end{aligned} \tag{1}$$

where $T \equiv T_{\mathrm{lab}} - k_g' Z$ measures time in the grating frame traveling at group velocity $k_g'^{-1}$, $k_j'' = d^2k/d\omega^2|_{\omega_j}$, $j = s, g$, are group-velocity dispersions (GVDs), and $\delta \equiv k_s' - k_g'$. In the following, without loss of generality [14], we assume velocity matching $\delta = 0$, which in our experiment is accomplished by carefully choosing $\omega_g$ and $\omega_s$ on opposite sides of the fiber zero GVD point. Assuming a continuous-wave (cw) grating propagating unchanged, i.e., $E_g(Z, T) = E_g(0, T) = 2P_g^{1/2}\cos(\Omega T)$, a signal of the form $E_s = [E_1 \exp(i\Omega T) + E_2 \exp(-i\Omega T)]\exp(i\beta Z)$ [where $E_{1,2} = E_{1,2}(Z, T)$ are slowly varying in $T$, and $\beta = 4\chi\Gamma + k_s''\Omega^2/2$ is a common phase shift] allows us to reduce the second of Eqs. (1) to the system

$$\begin{aligned} &i(\partial_Z + \delta k'\partial_T)E_1 + \Gamma E_2 + \chi(|E_1|^2 + 2|E_2|^2)E_1 = 0, \\ &i(\partial_Z - \delta k'\partial_T)E_2 + \Gamma E_1 + \chi(|E_2|^2 + 2|E_1|^2)E_2 = 0, \end{aligned} \tag{2}$$

which entail that $E_{1,2}$ suffer a group delay $2\delta k' = 2k_s''\Omega$ while coupling linearly and *resonantly* (i.e., without phase slippage) with coefficient $\Gamma = 2\chi P_g$, fixed by power $P_g$.

  

In the linear ($\chi = 0$) regime, cw solutions $E_{1,2}$ of Eqs. (2) with frequency detuning $\Delta\Omega$ from resonance ($\omega_s$) and related wave-number shift Re[$K$], viz., dependence $\exp(iKZ - i\Delta\Omega T)$, yield a dispersion relationship featuring two branches $K(\Delta\Omega) = K^{\pm} = \pm\sqrt{\Gamma^2 + (\delta k'\Delta\Omega)^2}$ separated by a forbidden $K$ gap $|K| < \Gamma$ [15]. The gap, displayed in Fig. 1(a) in terms of normalized quantities $k \equiv K/\Gamma$ and $\Delta\omega \equiv \Delta\Omega(\delta k'/\Gamma)$, originates from the features of the FWC process. In fact, owing to the fact that the eigenvalues of Eqs. (2) with $\chi = 0$ are $iK^{\pm}$, i.e., imaginary conjugated, the cw modes $E_{1,2}$ undergo periodic FWC with spatial frequency $|K(\Delta\Omega)|$ regardless of their detuning $\Delta\Omega$ [see insets of Fig. 1(a)]. The gap reflects the fact that such spatial frequency cannot decrease below its resonance value $|K(0)| = \Gamma$ (off-resonance the coupling period gets shorter), no matter whether the resonance is approached from above or below. This physics, common to other FWC schemes [10,11], is markedly different from that of BWC where the gap, shown for comparison in Fig. 1(b), appears in $\Omega$ and is related to linear wave solutions becoming evanescent (eigenvalues become real or $K$ purely imaginary) around Bragg resonance. This diversity has a major consequence in the *nonlinear* regime, where both $K$ gaps and $\Omega$ gaps become, in principle, accessible. FWC allows one, indeed, to excite nonlinear solutions in the gap by means of end firing, without requiring the huge power levels needed to bleach the high input reflectivity characteristic of BWC. Specifically, Eqs. (2) possess the following nonlinear *resonance soliton* solutions with in-gap wave number [6]

$$E_j = A_j\sqrt{(\Gamma/\chi)\eta(\tau)}\exp\{i[\phi_j(\tau) + kz - \delta\omega\tau]\}, \quad (3)$$

where $j = 1, 2$, and we set $z = \Gamma Z$ and $\tau = \gamma[T(\Gamma/\delta k') - vz]$, $\gamma = (1 - v^2)^{-1/2}$ being the Lorentz factor. The normalized parameters $v$ and $k$ ($|v|, |k| \leq 1$) fix the intensity $\eta(\tau)$ [$\eta(\pm\infty) = 0$] and chirp $\phi_j(\tau)$ profiles [6], and give the inverse soliton velocity in grating frame $k'_{\rm sol} = v\delta k'$ [16] and the soliton wave number $K = k\Gamma$ in frame $(z, \tau)$, respectively. While $v$ can be controlled by introducing the field imbalance $|E_1/E_2|^2 = (A_1/A_2)^2 = \sqrt{(1 + v)/(1 - v)}$, $k$ is related to the normalized soliton frequency $\delta\omega = \gamma vk$, and can be tuned by imposing a real-world offset $\Delta\omega_s = \delta\omega\gamma\Gamma/\delta k'$ from resonance $\omega_s$, i.e., $\omega_s \rightarrow \omega_s + \Delta\omega_s$. Solitons (3) exist in the whole region of the parameter space $(K/\Gamma)^2 + (k'_{\rm sol}/k''_s\Omega)^2 \leq 1$, which can be identified with the $K$ gap seen by the moving soliton [6]. Indeed, for $v = 0$ ($k'_{\rm sol} = 0$) this reduces to the aforementioned condition $|K| \leq \Gamma$. We focus our attention on the most intriguing case of $K$-gap center (perfect resonance, $k = \delta\omega = 0$) and still soliton ($v = 0$) requiring balanced input $A_2 = -A_1$. When such a soliton is launched along the fiber, the evolution is affected dramatically by the grating presence. To show this and validate the picture based on Eqs. (2), let us integrate numerically the NLSEs (1) with coefficients $k''_{s,g} = 10, -10.5$ ps$^2$/km and $\chi = 2.75$ W$^{-1}$ km$^{-1}$ characteristic of our fiber, and a soliton input corresponding to our choice of detuning $\Delta f = 2\Omega/(2\pi) = 1.64$ THz and $P_g = 4.5$ W (yielding signal pulses with power and duration characteristic of our experiment). When the grating is absent (or weak, $P_g \ll 4.5$ W) coupling is not sufficient to balance nonlinearity and group delay, and the signal dynamics is dominated essentially by the latter, as clearly shown in Fig. 2(a). While walking off, the two soliton

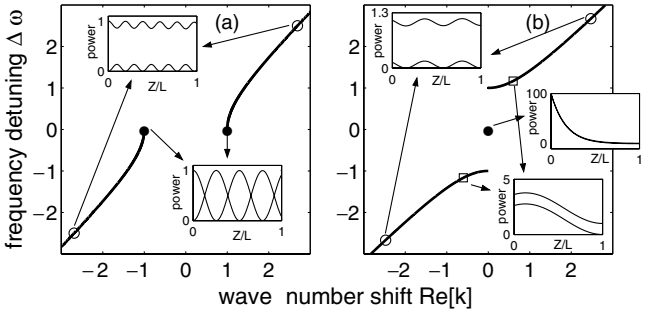


FIG. 1. (a) Dispersion relation $\Delta\omega$ vs Re[$k$] for FWC. Insets: Modal power evolutions $P_{1,2}(Z) = |E_{1,2}|^2$ for marked values of $|\Delta\omega|$ when mode 1 is launched [$P_{1,2}$ and $Z$ are in units of $P_1(0)$ and grating length $L$, $|\Gamma|L = 6$]. (b) As in (a) for BWC with insets relative to launching the forward mode 1 [$P_{1,2}$ in units of $P_1(L)$, $|\Gamma|L = 3$].

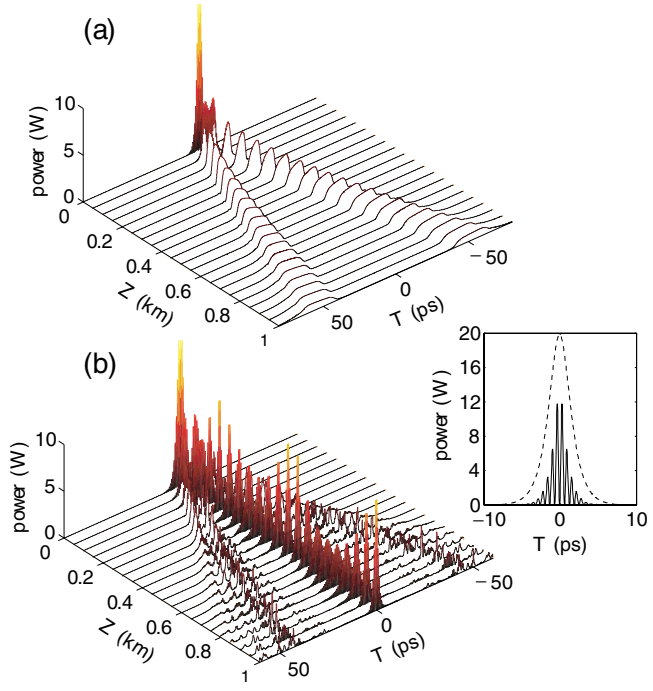


FIG. 2 (color online). Signal power evolution $|E_s(Z, T)|^2$ of a soliton input in the absence (a) or presence (b) of the grating wave $E_g$, as obtained from the NLSEs (1) with parameter values of our experiment (see text). The inset in (b) shows the output signal power compared with the input envelope (dashed line).

pulses also broaden due to the combined action of the GVD and the Kerr effect. Conversely, when the cw dynamic grating is raised up to the proper level ($P_g = 4.5$ W), linear (group-delay and coupling) and nonlinear effects mutually balance, and the group delay is suppressed via the formation of a still (in the grating frame) bound state [see Fig. 2(b)]. Within the bound-state envelope, short-scale oscillations of total power are due to mode beating (see inset). We emphasize that Eqs. (1) and the results of Fig. 2 account for the effects neglected by Eqs. (2), such as GVD-induced broadening, grating wave distortion occurring primarily via four-wave mixing (FWM, generations of sideband pairs at $\omega_g \pm n\Omega$, $n = 3, 5, \ldots$ [17]), as well as signal FWM at $\omega_s \pm n\Omega$. These effects are responsible for radiation of linear waves and bound-state oscillations, which, however, do not hamper the main signature of resonance trapping, namely, grating-induced group-delay cancellation.

The experimental setup used to detect such a phenomenon is displayed schematically in Fig. 3. The grating is excited by means of two long (540 ps FWHM) square pulses that ensure quasi-cw operation. These two pulses, at wavelengths $\lambda_{g1,g2} = 1538$ and 1551.1 nm, are synchronized since they are generated from two cw lasers injected in a fiber nonlinear loop mirror (NOLM) with dichroic couplers (WDM) along with a common intense control (switching) pulse from a Nd-YAG laser (120 ps, $\lambda = 1064$ nm). After amplification in an Er-doped fiber (EDFA) the plateau (peak) power of each of these grating waves can reach a maximum of about $P_g \simeq 18$ W, which yields a coupling coefficient (i.e., half $K$ gap) $\Gamma \simeq 10^{-3}\ \mathrm{cm}^{-1}$. In spite of this low value, the dynamical nature of the grating allows us to employ a long fiber ($L = 1$ km), which results in an efficient grating with high figure of merit $\Gamma L \simeq 100$. The two-color signal (soliton) waves are obtained by means of a versatile tunable laser source based on a spectroscopic filtering arrangement of fs pulses, releasing a pair of 3.9 ps pulses at $\lambda_{s1} = 1293.4$ nm and $\lambda_{s2} = 1302.6$ nm with peak power $|E_{1,2}|^2 = 3.8$ W. These wavelengths guarantee equalization of mean group velocities $k'_s = k'_g$. We can launch either some or all of such waves (with parallel polarization as well as overlapped in time), into our fiber sample (Teralight® by Alcatel) whose zero dispersion lies at $\lambda_{0D} = 1420$ nm. The chosen frequency $\Omega = 1.64\pi$ THz is high enough to yield a considerable group delay with moderate FWM, and yet such that $\Omega \ll \omega_s - \omega_g$ so that Eqs. (1) are accurate enough.

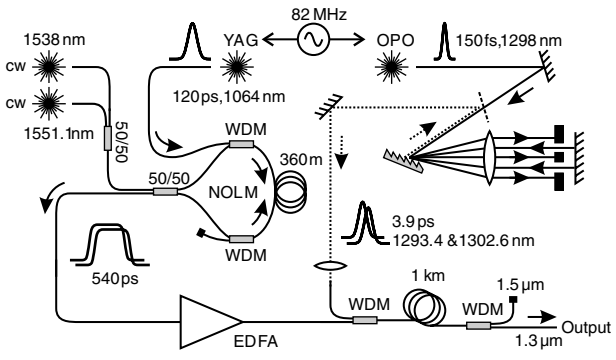


FIG. 3. Scheme of the experimental setup.

We have first checked the effectiveness of our dynamic grating scheme. To this end, we compare in Fig. 4 the output signal spectral density measured by launching only one signal wavelength, e.g., the slow mode at $\lambda_{s1}$ ($\omega_s + \Omega$), in the presence and absence of the grating, respectively. When $\lambda_{g1,g2}$ are copropagating with $\lambda_{s1}$, generation of $\lambda_{s2}$ ($\omega_s - \Omega$) is observed with power flowing from $\lambda_{s1}$ to $\lambda_{s2}$ until they exhibit comparable power. Such coupling is mediated by the grating since it disappears when $\lambda_{g1,g2}$ are not launched (see dashed-line spectrum). Owing to its nonlinear origin, coupling between the two signal modes can be interpreted as due to four-photon mixing amplifying $\omega_s \mp \Omega = (\omega_s \pm \Omega) \mp (\omega_g \pm \Omega) \pm (\omega_g \mp \Omega)$. The equalized mean group velocity $k'_s = k'_g$ allows for such mixing to be phase matched at second order in the expansion of $k(\omega)$, regardless of GVD values. Figure 4 shows also the presence of blueshifted (from $\lambda_{s1}$) radiation, which, along with redshifted (from $\lambda_{g2}$, not shown) twin photons, originates from broadband parametric amplification of noise due to spontaneous decay of pump photon pairs at $\omega_s + \Omega$ ($\lambda_{s1}$) and $\omega_g - \Omega$ ($\lambda_{g2}$), which is known to occur for pumps symmetrically located around $\lambda_{0D}$ [18]. Such fluorescence, however, has a minor impact on signal dynamics since (i) it does not involve resonant coupling (its mirror frequency is absent); (ii) it vanishes when $\lambda_{s1,s2}$ are both input.

Having proved the efficiency of the dynamic grating to couple the $\omega_s \pm \Omega$ modes, we have explored the solitonic regime. The resonance soliton trapping observed in the full nonlinear regime is illustrated by Fig. 5, which displays the temporal profile of the output signal intensity

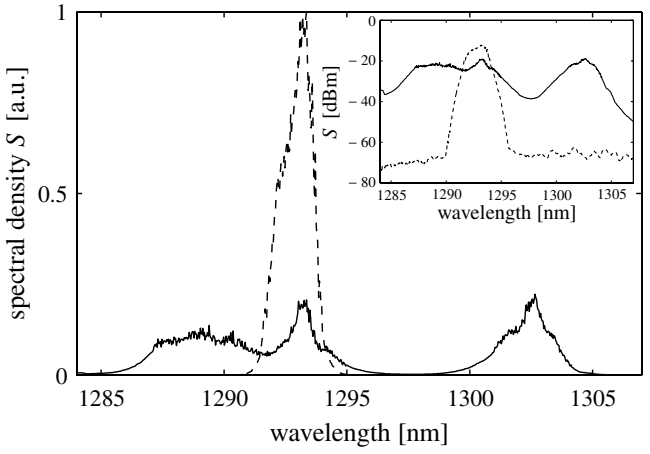


FIG. 4. Output spectral density $S(\lambda)$ (linear scale) measured with (solid line, $P_g = 16$ W) and without (dashed line) the input grating, when only the blueshifted ($\lambda_{s1}$) signal pulse is launched. The inset shows the corresponding log scale plot.

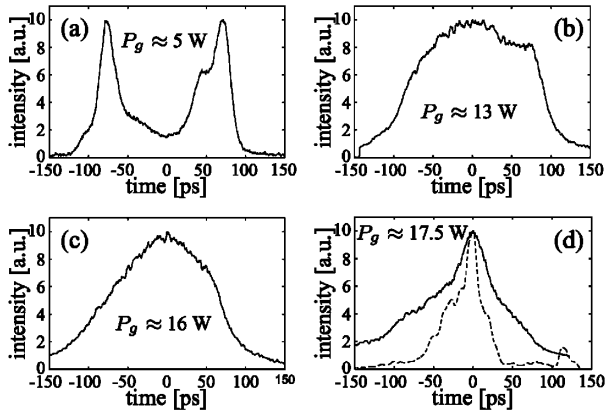


FIG. 5. Streak camera traces of the output signal obtained when two equally intense signal pulses are colaunched with grating waves of peak power $P_g$ [increasing from (a) to (d)]. The dashed curve in (d) shows the profile corresponding to the trapped signal, as obtained numerically from NLSEs (1).

measured by means of a streak camera (6 ps resolution) for increasing input grating power $P_g$. In Fig. 5(a), we show that at low grating power ($P_g = 5$ W) the two signal components emerge, slightly broadened (FWHM $\sim$ 20 ps) and well separated in time with a delay of 120 ps in good agreement with our linear estimate $\Delta t = 2k_s'' \Omega L \simeq 104$ ps. As the grating power is increased to 13 W [Fig. 5(b)] and 16 W [Fig. 5(c)] the group delay of the two pulses reduces progressively, until eventually the two pulses merge at $P_g = 17.5$ W to form a bound state, similar to what is shown in Fig. 2(b). The beating oscillation with period $\sim$0.6 ps expected under the envelope is beyond resolution of our apparatus.

Although the transition from dispersive behavior to group-delay suppression in Fig. 5 is incontrovertible, it occurs at grating powers considerably higher than the value $P_g \sim 4.5$ W employed in Fig. 2 and expected from theory to yield trapping of soliton pulses with duration and peak power characteristic of our setup. We attribute this quantitative discrepancy mainly to the fact that the input signal pulses possess neither the chirps [$\phi_{1,2}$ in Eq. (3)] nor the relative phase of the ideal soliton. Under these conditions, we find that linear radiation becomes more significant, and one needs to supply substantially more power than that needed with ideal soliton input as in Fig. 2(b). Further waste of effective energy is due to FWM. Note, however, that the measured level of leading-order FWM at $\omega_{g,s} \pm 3\ \Omega$ is at least 20 dB below the level of the main modes, thus suggesting a moderate impact. Nevertheless, in order to fit the experiment more closely, we have run a simulation based on Eqs. (1), which account for the exact shape of the grating pulses at 17.5 W, FWM effects, as well as the additional effect of losses (0.2 dB/km), stimulated Raman scattering (causing energy flow towards long grating and signal wavelengths), and the detection apparatus response. The result displayed in Fig. 5(d) shows a reasonable agreement with the experimental data, supporting the basic validity of the proposed picture.

In summary, we have reported the first evidence of pulse trapping in a periodic system with a photoinduced gap in wave number. Our dynamic grating allows efficient trapping to be observed right on resonance, which is hardly possible with counterpropagating modes.

This research is supported by the interuniversity attraction pole program (OSTC, Belgium). S. C. and S. T. acknowledge support from FNRS, Belgium, and MIUR, Italy, respectively.

[1] *Nonlinear Photonics Crystals* (Springer-Verlag, Berlin, 2003), edited by R. E. Slusher and B. J. Eggleton.
[2] B. J. Eggleton *et al.*, Phys. Rev. Lett. **76**, 1627 (1996); N. G. R. Broderick *et al.*, Phys. Rev. Lett. **79**, 4566 (1997).
[3] J. W. Fleischer, M. Segev, N. K. Efremidis, and D. N. Christodoulides, Nature (London) **422**, 147 (2003).
[4] W. Chen and D. L. Mills, Phys. Rev. Lett. **58**, 160 (1987).
[5] A. B. Aceves and S. Wabnitz, Phys. Lett. A **141**, 37 (1989); D. N. Christodoulides and R. I. Joseph, Phys. Rev. Lett. **62**, 1746 (1989).
[6] C. Conti and S. Trillo, Phys. Rev. E **64**, 036617 (2001).
[7] S. John and J. Wang, Phys. Rev. Lett. **64**, 2418 (1990); D. Barday and M. Remoissenet, Phys. Rev. B **41**, 10 387 (1990); P. J. Y. Louis, E. A. Ostrovskaya, C. M. Savage, and Y. S. Kivshar, Phys. Rev. A **67**, 013602 (2003).
[8] C. Conti, S. Trillo, and G. Assanto, Phys. Rev. Lett. **78**, 2341 (1997); A. E. Kozhekin, G. Kurizki, and B. Malomed, Phys. Rev. Lett. **81**, 3647 (1998); H. G. Winful and V. Perlin, Phys. Rev. Lett. **84**, 3586 (2000).
[9] S. John and N. Aközbek, Phys. Rev. Lett. **71**, 1168 (1993).
[10] S. Trillo, S. Wabnitz, and G. I. Stegeman, IEEE J. Lightwave Technol. **6**, 971 (1988); S. Trillo *et al.*, IEEE J. Quantum Electron. **QE-25**, 104 (1989); J. N. Kutz, B. J. Eggleton, J. B. Stark, and R. E. Slusher, IEEE J. Sel. Top. Quantum Electron. **3**, 1232 (1997). Drawbacks of such schemes are scarcely reproducible fabrication (FWC of polarization modes), or difficulty to control launching conditions (FWC of higher-order modes).
[11] S. Wabnitz, Opt. Lett. **14**, 1071 (1989).
[12] S. Pitois, M. Haelterman, and G. Millot, J. Opt. Soc. Am. B **19**, 782 (2002).
[13] G. P. Agrawal, Phys. Rev. Lett. **59**, 880 (1987).
[14] $\delta$ can be removed by means of the transformation $E_s \rightarrow E_s \exp(i\Delta T - i\Delta\delta Z)$, where $\Delta = \delta/k_s''$ makes the group velocities at $\omega_g$ and the new frequency $\omega_s + \Delta$ equal.
[15] Though obtained in the moving frame, the $K$ gap persists in the laboratory frame, where the relation $K(\Delta\Omega)$ should be replaced by $K_{\rm lab}(\Delta\Omega)$ with $K_{\rm lab} = K + k_g' \Delta\Omega$.
[16] The soliton velocity in laboratory frame $V_{\rm sol} = (k_g' + k_{\rm sol}')^{-1}$ turns out to bounded by the linear velocities $V_{\pm\Omega} = (k_g' \pm \delta k')^{-1}$ of $\omega_s \pm \Omega$ modes.
[17] J. R. Thompson and R. Roy, Phys. Rev. A **43**, 4987 (1991); **44**, 7605 (1991); S. Trillo, S. Wabnitz, and T. A. B. Kennedy, Phys. Rev. A **50**, 1732 (1994).
[18] J. M. Chávez Boggio, S. Tenenbaum, and H. L. Fragnito, J. Opt. Soc. Am. B **18**, 1428 (2001).